Journal of
Instrumentation



# Progress in experimental setup and reconstruction algorithms in RIPTIDE



Jinst

Published by IOP Publishing for Sissa Medialab

Received: *September 29, 2025*
Revised: *November 17, 2025*
Accepted: *November 19, 2025*
Published: *December 19, 2025*

26th International Workshop on Radiation Imaging Detectors
Bratislava, Slovakia
6–10 July 2025

# Progress in experimental setup and reconstruction algorithms in RIPTIDE

**Samuele Lanzi**,[a,b,*] **Patrizio Console Camprini**,[b] **Francesco Giacomini**,[a] **Cristian Massimi**,[c,b] **Alberto Mengarelli**,[c] **Claudia Pisanti**,[c,b] **Riccardo Ridolfi**,[c,b] **Roberto Spighi**[c] **and Mauro Villa**[c,b]

[a] *INFN-CNAF, Viale Berti Pichat 6/2, Bologna, Italy*
[b] *Department of Physics and Astronomy, University of Bologna, Viale Berti Pichat 6/2, Bologna, Italy*
[c] *Istituto Nazionale di Fisica Nucleare (INFN), Viale Berti Pichat 6/2, Bologna, Italy*

*E-mail:* samuele.lanzi@cnaf.infn.it

Abstract: Tracking imaging systems have evolved from manual analysis to advanced photodetectors, such as SiPM arrays and CMOS cameras, enabling the conversion of scintillation light into digital data for precise physical measurements. This study presents RIPTIDE, a recoil-proton track imaging system for fast neutron detection. The system employs a plastic scintillator where fast neutrons scatter elastically with protons, producing scintillation light. The generated signal is then captured by an optimized optical setup comprising a lens system, a Microchannel Plate (MCP), and a high-frame-rate CMOS sensor. Monte Carlo simulations have been conducted to explore the detector performance and to generate image datasets for testing reconstruction algorithms. These algorithms aim to infer neutron tracks by analyzing the direction and range of recoil protons. Additionally, a deep neural network is implemented to correct optical aberrations introduced by the lens system, enhancing the accuracy of proton range measurements. The experimental setup is currently under construction, and initial acquisitions have been performed to validate the Monte Carlo simulations. Results obtained in the laboratory on the detection of minimun ionizing particles will be presented.

Keywords: Detector modelling and simulations I (interaction of radiation with matter, interaction of photons with matter, interaction of hadrons with matter, etc); Neutron detectors (cold, thermal, fast neutrons); Photon detectors for UV, visible and IR photons (solid-state) (PIN diodes, APDs, Si-PMTs, G-APDs, CCDs, EBCCDs, EMCCDs, CMOS imagers, etc); Scintillators, scintillation and light emission processes (solid, gas and liquid scintillators)

*Corresponding author.



https://doi.org/10.1088/1748-0221/20/12/C12030

2025 JINST 20 C12030

## Contents



## 1 Introduction

Neutron detector technology is less mature than charged particle tracking, with only a few concepts based on neutron-proton (n-p) elastic scattering reported in the literature [1–5]. Systems such as SONTRAC [6] and MONDO [2, 7] rely on multiple scattering in scintillating fiber matrices, but face challenges in terms of readout, data transfer, and detection thresholds.

We propose a new detector concept, RIPTIDE (RecoIl Proton Track Imaging DEtector) [8–12], which uses a monolithic plastic scintillator coupled to a lens system and an image intensifier. Its key innovation is the reconstruction of recoil-proton tracks in space and time from scintillation light, enabling neutron spectrometry and real-time analysis of energy deposition.

This work presents Geant4 simulations of n-p scattering and optical photon transport, optical system studies supported by laboratory tests, and first results obtained with the HiCAM FLUO camera [13], which integrates the image intensifier, phosphor screen, and a fast CMOS sensor.

## 2 Detector concept

Figure 1 illustrates the principle of neutron detection in RIPTIDE. The process begins when an incoming neutron undergoes elastic scattering, predominantly with hydrogen nuclei in the organic scintillator. In such interactions, part of the neutron kinetic energy is transferred to recoil protons, which subsequently deposit energy along their paths through ionization, with the maximum deposition occurring at the Bragg peak [14]. Although scattering with carbon nuclei is possible and their cross section is of a similar magnitude, recoil carbon nuclei travel shorter paths in the scintillator, making them invisible.

The deposited energy excites the scintillator, producing scintillation photons that are emitted isotropically throughout the material. Two independent optical arms, placed along orthogonal projections, collect this light. Each arm employs a lens system that focuses the photons onto a microchannel plate (MCP) image intensifier [15], providing amplification of about $10^6$ while



2025 JINST 20 C12030

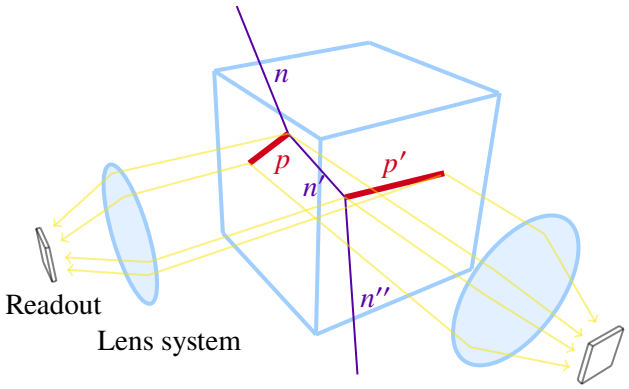


**Figure 1.** Schematic of the RIPTIDE detector concept.

preserving the spatial distribution of the optical signal. The intensified images are then recorded by fast CMOS sensors, which capture the spatial patterns needed for subsequent proton track analysis.

The recorded two-dimensional projections from the two orthogonal optical systems were combined to reconstruct the full three-dimensional trajectory of the recoil proton inside the scintillator volume. The foundation for reconstructing the neutron momentum lies in two-body kinematics. In the case of a single neutron-proton scattering event, the incident neutron kinetic energy $E_n$ can be determined from the recoil proton kinetic energy $E_p$ and its scattering angle $\theta_p$ with respect to the neutron direction as

$$E_n = \frac{E_p}{\cos^2 \theta_p}. \tag{2.1}$$

If the direction of the neutron source is known, this single scattering is sufficient to estimate $E_n$.

In contrast, if the neutron source direction is unknown, a double-scattering event must be considered. In this case, the scattering angle is obtained geometrically from the positions of the two interaction vertices. Applying eq. (2.1) to both vertices makes it possible to fully reconstruct both the energy and the incoming direction of the neutron [16, 17].

Finally, the recoil proton energy $E_p$ is determined from the length of the track, or *range* ($R$). The range-energy relation in the scintillator material follows

$$R(E) = \alpha E^p, \tag{2.2}$$

where $\alpha$ and $p$ are material-dependent parameters [16].

## 3 Monte Carlo simulation

The detection concept proposed in this study has been supported by Monte Carlo simulations based on the Geant4 toolkit [18]. The simulation architecture was designed following a modular and flexible paradigm. The detector geometry and material composition are defined at run-time through GDML (Geometry Description Markup Language) files. This implementation choice offers significant advantages: it enables the reuse of simulation code for different geometric configurations and allows for parametric optimization of the detector without modifying the source code.



2025 JINST 20 C12030

As an example of the geometry implemented, we consider the configuration described in section 2. A scintillator cube with dimensions of $60 \times 60 \times 60$ mm$^3$ was modeled using polyvinyltoluene, representative of the BC-408 material. Its properties, retrieved from the NIST database [19], are available within the Geant4 material libraries under the name `G4_PLASTIC_SC_VINYLTOLUENE`. The material is characterized by a stoichiometric C/H ratio of 9/10, a density of 1.032 g/cm$^3$, and a mean ionization energy of 64.7 eV.

Simulations were performed using standard Geant4 physics lists, which include models for electromagnetic and hadronic interactions. Optical photon generation and transport were enabled by using dedicated optical physics processes. According to the BC-408 datasheet [20], $10^4$ optical photons were generated per MeV of energy deposited along the proton tracks and then propagated within the plastic scintillator.

As recoil protons traverse the plastic scintillator, the energy they deposit leads to the production of optical photons. These photons are collected by an optical system composed of two plano-convex lenses with focal lengths of 75 mm and 60 mm, respectively, each with a diameter of approximately 50 mm. The lenses are arranged in a *Ramsden eyepiece* configuration, with the lens of longer focal length placed closer to the sensor.

In the simulation, the optical system was optimized by systematically varying two parameters: the distance from the scintillator to the first lens and the distance from the second lens to the sensor. The performance of each configuration was evaluated by analyzing the image of a simulated point-like light source. The sharpness of the focus was quantified by measuring the Full Width at Half Maximum (FWHM) of the resulting light distribution on the sensor (i.e., the point spread function). The configuration that minimized the FWHM, thus providing the highest spatial resolution, was chosen as the optimum.

The best configuration was found for a scintillator-lens distance of 110 mm and a lens-sensor distance of 41 mm. This setup provides a depth of field of approximately 30 mm, a field of view of $50 \times 50$ mm$^2$, and a magnification factor of about $1:3$. In the Geant4 simulation, the trajectories of the optical photons are tracked, and their interactions with the sensor surface are recorded. The resulting hits are stored in ROOT files as two-dimensional histograms, which serve as input for the subsequent analysis figure 2.

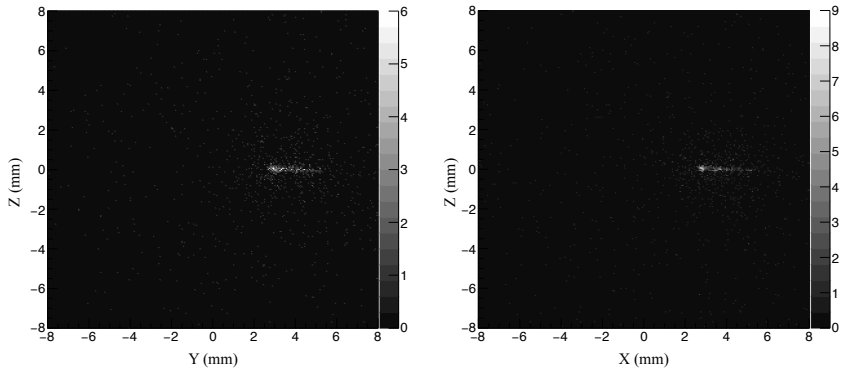


**Figure 2.** Example of Monte Carlo simulation output: scintillation light produced by a 30 MeV recoil proton as detected on the sensor.



2025 JINST 20 C12030

## 4 Reconstruction techniques

The reconstruction of recoil proton tracks is performed through a multi-step approach that combines classical computer vision methods with deep learning techniques. These techniques are described in detail and quantitatively in [21]; here we focus instead on outlining the underlying logic of the reconstruction chain. The adopted strategy enables the determination of both the direction and the energy of the incident neutron, and can be divided into three main phases:

1. *Extraction of the proton direction:* the two-dimensional projection of the recoil proton track on the sensor is first processed using the Hough transform, which provides an estimate of the angular direction of the trajectory. The orientation along this direction is then determined by analyzing the asymmetry of the energy deposition profile, i.e. the Bragg curve. This is achieved through a moment analysis based on the skewness, which allows for the identification of the start and end points of the proton track.

2. *Correction of optical distortions and range estimation:* the imaging system introduces optical distortions that affect the observed track morphology. To correct for these effects, a convolutional neural network based on the U-Net architecture is employed. The network restores the original track shape into a binary image, from which the track length can be extracted.

3. *Track reconstruction and neutron energy estimation:* the 3d vector of the recoil proton is obtained by combining the information extracted from two stereoscopic projections. Once the track length is determined, the proton range is converted into kinetic energy by means of an empirical power-law relationship calibrated on Monte Carlo simulations. This procedure enables the reconstruction of the incident neutron energy with a resolution of 5% for mono-energetic neutrons at 50 MeV.

## 5 Experimental setup

The sensitivity of the detection system was validated using minimum ionizing particles (MIPs). Although MIP detection is not the primary goal of RIPTIDE, it serves as a useful benchmark for the system detection capability. MIPs deposit less energy per unit length compared to recoil protons from neutron elastic scattering, resulting in weaker scintillation light.

Two types of scintillators were tested: the plastic scintillator BC-408, which provides a light yield of about $10^4$ photons/MeV, and the denser CsI(Tl), which offers a yield approximately five times higher. The choice of BC-408 as the primary scintillator material for RIPTIDE is motivated by several factors. While CsI(Tl) offers higher light yield, BC-408 provides distinct advantages for neutron detection: its high hydrogen content maximizes the probability of neutron-proton elastic scattering, it exhibits a faster decay time (2.1 ns compared to 680 ns for CsI(Tl)) which is crucial for high count rate scenarios and temporal resolution, and its lower density results in longer proton ranges, facilitating track reconstruction and direction determination. Additionally, BC-408 can be manufactured in larger volumes at lower cost, making it practical for scaling up the detector. However, for the present validation tests with minimum ionizing particles, CsI(Tl) is expected to provide better visibility due to its superior light yield.



2025 JINST 20 C12030

A mirror, positioned at a 45° angle beside the scintillator, allowed for a simultaneous lateral view, enabling the reconstruction of the three-dimensional track. The total scintillation light is collected by the optical system described in section 3 and subsequently detected by the HiCAM FLUO camera. A schematic of the experimental setup is shown in figure 3.

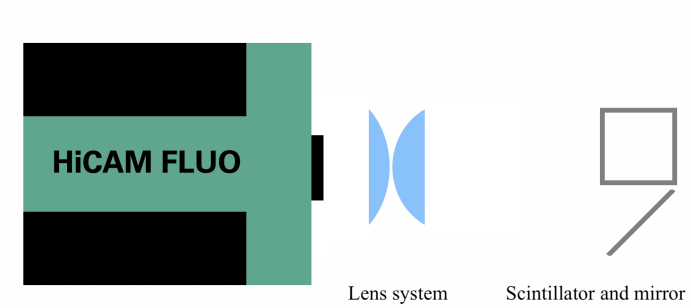


**Figure 3.** Schematic representation of the experimental setup. Scintillation light produced in the target (BC-408 or CsI(Tl)) is collected by an optical system and imaged onto the HiCAM FLUO single-photon sensitive camera.

The HiCAM FLUO is optimized for single-photon imaging and integrates several internal components. At the front end, it employs a microchannel plate (MCP) image intensifier with an 18 mm diameter borosilicate input window and a GaAsP photocathode, which is particularly suitable for our application thanks to its high quantum efficiency in the visible range, peaking at about 40% between 400 and 650 nm. The system also provides an exceptionally low equivalent background illumination (EBI) of $1.0 \times 10^{-12}$ lm/cm$^2$, effectively minimizing noise in low-light conditions. The amplified electron signal is then converted into visible light on a P46 phosphor screen and subsequently coupled via fiber optics to a Cyclone-2000-M fast CMOS camera, ensuring efficient signal transfer. Finally, the camera is connected to the acquisition computer through a Coaxlink Quad CXP-12 frame grabber, enabling high-speed data transfer with frame rates of up to 2166 Hz.

## 6 Experimental results and discussion

Using the experimental setup described in section 5, data were acquired with both the BC-408 and the CsI(Tl) scintillators exposed to minimum ionizing particles (MIPs).

In figure 4, the left part shows the image of a track produced by a cosmic muon crossing the CsI(Tl) scintillator, while the right part displays the corresponding mirrored track. In the case of the BC-408 scintillator, only localized signal enhancements were observed in some images; however, at this stage, no clear track-like structures could be identified.

These preliminary results demonstrate that MIPs can be directly imaged in CsI(Tl), owing to its higher scintillation yield. In contrast, the BC-408 plastic scintillator emits about five times fewer photons, making MIP detection challenging. However, protons have a much larger stopping power than MIPs and deposit significantly more energy per unit path length. As a consequence, the scintillation light produced in BC-408 by proton tracks is expected to exceed the detection threshold of our system. Thus, while muon tracks are more readily observed in CsI(Tl), BC-408 remains well suited for detecting the proton-induced tracks that constitute the main signal of this study.



2025 JINST 20 C12030

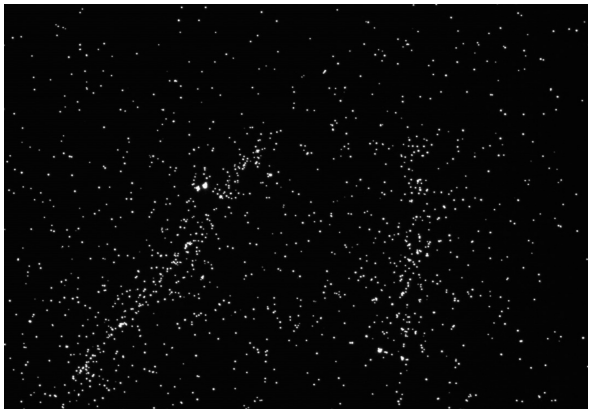

**Figure 4.** Example of a MIP event: the left panel shows a track produced by a cosmic muon in the CsI(Tl) scintillator, while the right panel displays the corresponding mirrored image.

## 7 Conclusions

In this work we presented the RIPTIDE detector concept, a novel system for fast neutron detection based on the direct imaging of recoil-proton tracks in a plastic scintillator. Monte Carlo simulations demonstrated the feasibility of reconstructing neutron kinematics through stereoscopic optical projections, supported by advanced image processing and deep learning techniques for track reconstruction.

A first laboratory characterization was carried out with minimum ionizing particles using both BC-408 and CsI(Tl) scintillators. While muon tracks were clearly observed in CsI(Tl), only localized signal excesses were detected in BC-408, in line with expectations given the different light yields. These results confirm the sensitivity of the system and indicate that proton-induced tracks, which deposit significantly more energy per unit length than MIPs, will be detectable in BC-408.

Ongoing developments include a systematic analysis of the experimental data and the refinement of the optical and reconstruction algorithms.

## References


[1] J. Hu et al., *Recoil-proton track imaging as a new way for neutron spectrometry measurements*, *Sci. Rep.* **8** (2018) 13363.

[2] S.M. Valle et al., *The MONDO project: A secondary neutron tracker detector for particle therapy*, *Nucl. Instrum. Meth. A* **845** (2017) 556.

[3] E. Gioscio et al., *Development of a novel neutron tracker for the characterisation of secondary neutrons emitted in Particle Therapy*, *Nucl. Instrum. Meth. A* **958** (2020) 162862.

[4] G. Wang et al., *Optical Method Based on a Gaseous Scintillator for Neutron Energy Spectrum Measurements*, *J. Appl. Spectrosc.* **87** (2020) 911.

[5] R.S. Miller et al., *SONTRAC: An imaging spectrometer for MeV neutrons*, *Nucl. Instrum. Meth. A* **505** (2003) 36.

[6] J.G. Mitchell et al., *Development of the Solar Neutron TRACking (SONTRAC) Concept*, *PoS* **ICRC2021** (2021) 1250.

[7] M. Marafini et al., *MONDO: a neutron tracker for particle therapy secondary emission characterisation*, *Phys. Med. Biol.* **62** (2017) 3299.




2025 JINST 20 C12030

[8] A. Musumarra et al., *RIPTIDE: a novel recoil-proton track imaging detector for fast neutrons*, 2021 *JINST* **16** C12013 [arXiv:2109.11543].

[9] C. Massimi et al., *"RIPTIDE" — an innovative recoil-proton track imaging detector*, 2022 *JINST* **17** C09026.

[10] P.C. Camprini et al., *A proton-recoil track imaging system for fast neutrons: the RIPTIDE detector*, 2023 *JINST* **18** C01054 [arXiv:2210.17431].

[11] C. Pisanti et al., *Riptide: a proton-recoil track imaging detector for fast neutrons*, 2024 *JINST* **19** C02074 [arXiv:2312.06676].

[12] C. Pisanti et al., *Sensor performance evaluation for candidate photon readout systems in the RIPTIDE detector*, *Appl. Radiat. Isot.* **225** (2025) 112077.

[13] Lambert Instruments, *HiCAM FLUO — high-speed fluorescence imaging camera*, https://lambertinstruments.com/products/hicam-fluo (2024).

[14] W.H. Bragg and R. Kleeman, *XXXIX. On the α particles of radium, and their loss of range in passing through various atoms and molecules*, *Philos. Mag.* **10** (1905) 318.

[15] J.L. Wiza, *Microchannel plate detectors*, *Nucl. Instrum. Meth.* **162** (1979) 587.

[16] J.F. Ziegler, M.D. Ziegler and J.P. Biersack, *SRIM — The stopping and range of ions in matter (2010)*, *Nucl. Instrum. Meth. B* **268** (2010) 1818.

[17] G.F. Knoll, *Radiation Detection and Measurement*, 4th ed., John Wiley & Sons (2010).

[18] GEANT4 collaboration, *GEANT4 — A Simulation Toolkit*, *Nucl. Instrum. Meth. A* **506** (2003) 250.

[19] National Institute of Standards and Technology (NIST), *Atomic Weights and Isotopic Compositions — Relative Atomic Masses*, https://www.nist.gov/pml/atomic-weights-and-isotopic-compositions-relative-atomic-masses.

[20] Eljen Technology, *General Purpose Plastic Scintillators EJ-200, EJ-204, EJ-208, EJ-212*, https://eljentechnology.com/products/plastic-scintillators/ej-200-ej-204-ej-208-ej-212.

[21] S. Lanzi et al., *Scintillating light track reconstruction for fast neutron detection based on deep-learning techniques*, *PoS* **ISGC2025** (2025) 021.

2025 JINST 20 C12030